Maejo Int. J. Sci. Technol. **2020**, *14*(02), 119-129

Maejo International Journal of Science and Technology

ISSN 1905-7873
Available online at www.mijst.mju.ac.th

Full Paper

Subsurface soil characterisation at Guar Kepah, Kedah Tua (Malaysia) using electrical resistivity tomography for archaeological purpose

Sabiu B. Muhammad [1, 3, *], Rosli Saad [1], Mokhtar Saidin [2], Nordiana M. Mustaza [1], Rais Yusoh [1], Yusuf A. Sanusi [3], Yakubu M. Samuel [1, 4] and Mustapha A. Mohammed [1, 5]

[1] Geophysics Section, School of Physics, Universiti Sains Malaysia, 11800 Penang, Malaysia
[2] Centre for Global Archaeological Research, Universiti Sains Malaysia, 11800 Penang, Malaysia
[3] Department of Physics, Usmanu Danfodiyo University, Sokoto, PMB 2346 Sokoto, Nigeria
[4] School of Science and Technology, Federal Polytechnic, PMB 1006 Damaturu, Nigeria
[5] Department of Physics, Federal University Lafia, PMB 146 Lafia, Nigeria
* Corresponding author e-mail: sabiubala@gmail.com

Received: 12 April 2019 / Accepted: 13 May 2020 / Published: 19 May 2020

Abstract: Characterisation of subsurface soil at Guar Kepah, Kedah Tua (Malaysia) was carried out using electrical resistivity tomography for shallow archaeological investigation. Apparent resistivity data were acquired using ten profiles and one additional profile at the edge of an already excavated portion of the study area for correlation of soil types. Subsurface resistivity values obtained in the study area led to four distinct soil types. The first (very-low resistivity of < 20 Ωm) was wet clay; the second (low resistivity of 20-100 Ωm) was sandy clay; the third (intermediate resistivity of 100-200 Ωm) consisted of shell flakes mixed with sandy clay; and sand (high resistivity of > 200 Ωm) was confirmed in the fourth type. A very-low resistivity (< 20 Ωm) anomaly was identified in the resistivity tomograms of the ten profiles, interpreted as wet clay materials associated with archaeological remains.

Keywords: electrical resistivity tomography, soil type, resistivity anomaly, archaeological sites, Malaysia

INTRODUCTION

Exploration geophysics is primarily concerned with the investigation of earth's crust and its near-surface features for practical and economic objectives [1]. Detection of structures beneath the earth's surface depends upon those properties which distinguish them from the surrounding media. For example, the seismic method takes advantage of contrast in the velocity of acoustic waves as they propagate through the subsurface to distinguish between rocks and soil of varied materials [2].

Maejo Int. J. Sci. Technol. **2020**, *14*(02), 119-129

In the magnetic method magnetic susceptibility contrast is used to differentiate underground materials [3-4]. In the gravity method variations in density are used to identify targets of interest [5-6]. Ground penetrating radar is also another powerful tool used for very shallow materials, mainly when subsurface structures are distinguishable by their conductivity or reflectivity to radar pulses [7].

In the same manner the electrical resistivity method uses contrast in resistivity distribution to distinguish between subsurface materials [8]. The method injects current into the ground via two electrodes. Electric potential is then measured using another set of electrodes in the neighbourhood of the current flow. Since the magnitude of the current applied is usually known, it is therefore possible to calculate the effective underground resistivity. This particularly makes it theoretically superior to all other electrical methods, as quantitative results can be obtained through the application of a controlled current source of specific dimensions [9].

Resistivity method has been applied to many practical problems such as those in engineering and environment [10-12], hydrological investigations [13], exploration of mineral deposits [14] and the detection of buried metallic objects and cavities [15]. It has equally been proved useful in hydrocarbon exploration, forensic studies [1] and regional geological investigations [16]. Resistivity method was also used for archaeological investigations [17-19]. The method has progressively developed especially in data acquisition and processing [20-22] although other methods have previously been utilised for similar objectives [5, 23-26]. Resistivity method gives sharp images of an anomaly with sharp contrast, devoid of ambiguity in interpretation and resolves both horizontal and vertical changes.

Recently, a research study traced a human skeleton surfaced at Guar Kepah area [27]. The work has further suggested the presence of buried shell mounds, indicative of more skeletons in the area, which is expected to be subjected to massive excavation activities in search of human and other forms of buried archaeological remains. Therefore, adequate knowledge of the soil types to be encountered in the process cannot be overemphasised. The objective of this research is to characterise the different subsurface soil types in the study area based on resistivity values. Potential buried ancient artefacts mainly in the form of consolidated clay if present may be well resolved by this method.

GEOLOGICAL SETTING OF STUDY AREA

Guar Kepah is an integral part of Seberang Perai, located on a stranded beach ridge deposited around mid-Holocene sea transgression, which is about 4,000-5,000 years ago [28]. Seberang Perai area is underlain by pre-Quaternary granite and sedimentary rocks of Sungai Petani and Mahang Formations [29]. The coastal areas are underlain by Simpang, Gula and Beruas Formations of Quaternary age [30]. The Simpang Formation is composed of gravel, sand, clay, silt and peat by terrestrial fluvial deposit. The Gula Formation is also made of silt, clay, sand, gravel and peat. Shell fragments are often deposited within an estuarine and shallow marine environment. The Beruas Formation consists of clay, silt, sand, gravel and occasional peat. Figure 1 shows a surface geological map of Guar Kepah area. Some of the localised geological features identified in the study area during field observation are shown in Figure 2.

Maejo Int. J. Sci. Technol. **2020**, *14*(02), 119-129

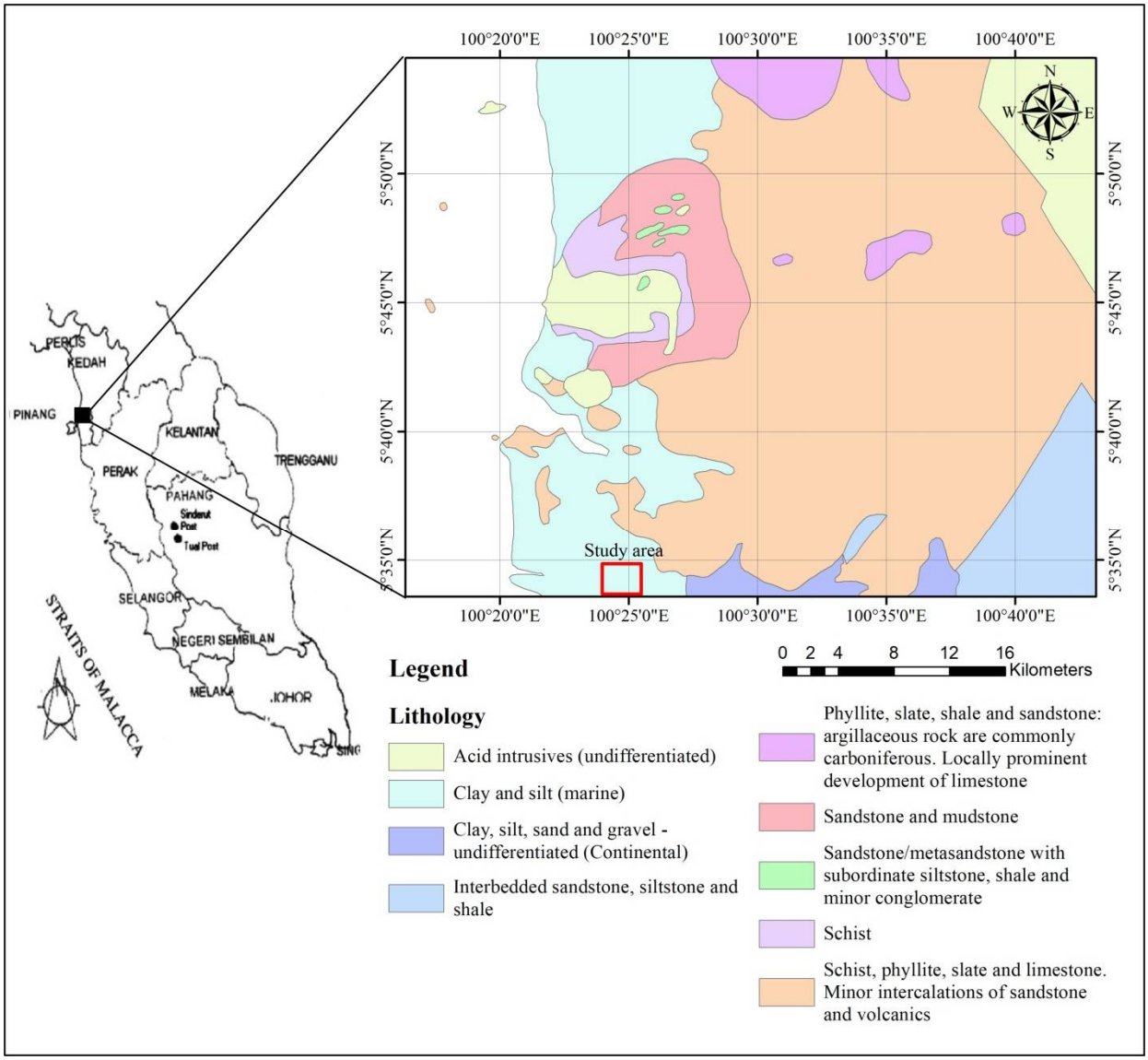

Figure 1. Geological map of Guar Kepah showing the study area [17]

PRINCIPLE OF RESISTIVITY METHOD

The principle guiding the resistivity method is Ohm's Law, which states that electric current (I) in a conducting medium is directly proportional to potential difference (V) across the conductor: $V=IR$, where R is the resistance of medium (ohm, Ω). For a uniform material, its resistance is directly proportional to its length (L) and inversely proportional to its area of cross-section (A). This can be expressed mathematically as $R=\rho(L/A)$, where ρ is proportionality constant, known as the resistivity of the material.

In the resistivity method artificially generated current is injected into the ground through point electrodes (C1 and C2). Electric potential is then measured using a pair of electrodes (P1 and P2) near the current flow (Figure 3). It is therefore possible to calculate the apparent resistivity since the magnitude of current applied is known.

Maejo Int. J. Sci. Technol. **2020**, *14*(02), 119-129

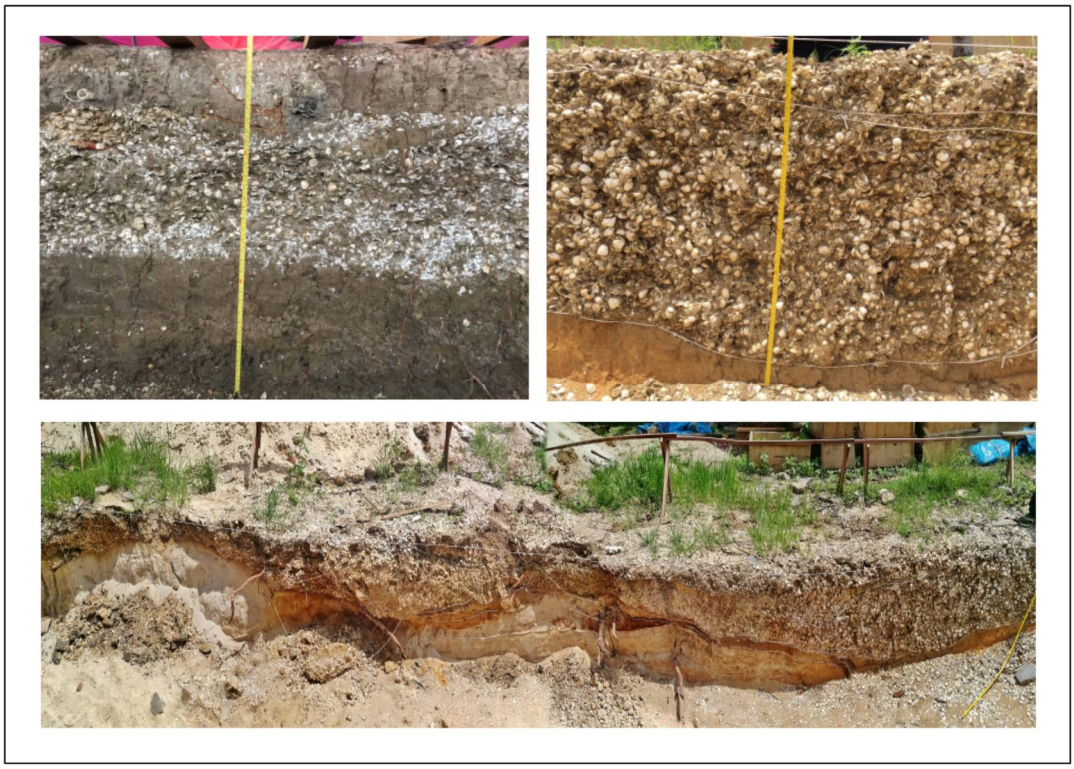

Figure 2. Localised geological features in study area

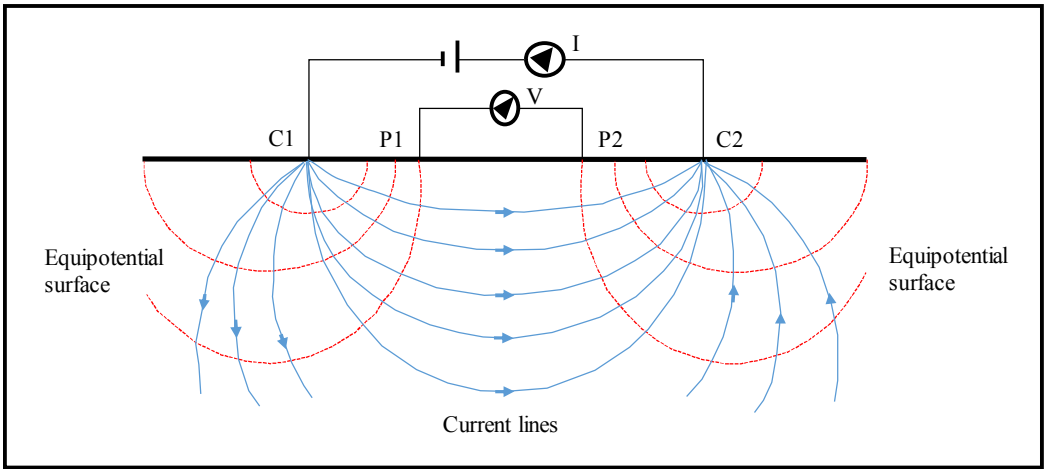

Figure 3. Four-point electrode configuration with current and potential [31]

True resistivity estimated from the inversion of the measured apparent resistivity can be related to several other geological parameters or factors such as mineral content, porosity, pore fluid type and degree of saturation, leading to the identification of geological features. The resistivity of buried materials may vary widely depending on these factors. Metallic ores, for example, can have a resistivity value of 10^{-5} Ωm compared to about 10^{8} Ωm obtained for dry marble. Resistivity values of most other common materials fall between these extreme values (Table 1).

Maejo Int. J. Sci. Technol. **2020**, *14*(02), 119-129

Table 1. Resistivity of some common rocks and soil materials [1]

Material	**Resistivity, ρ (Ωm)**
Granite	$3 \times 10^2 – 10^6$
Granite (weathered)	$3 \times 10 – 5 \times 10^2$
Schist (calcareous and mica)	$20 – 10^4$
Quartzite	$10^3 – 10^5$
Basalt	$1 – 10^5$
Graphite	$10^{-4} – 10^{-2}$
Graphitic Schist	$10^{-1} – 50$
Sandstone	$1 – 7.4 \times 10^8$
Limestone	$10 – 10^7$
Clay	$1 – 10^2$
Alluvium	$1 – 10^3$
Consolidated shale	$20 – 2 \times 10^3$
Sand and gravel	$10 – 10^4$

MATERIALS AND METHODS

A ground resistivity survey was conducted using ten profiles (L1-L10) arranged at 1-m constant profile spacing to map the study area. The data were also acquired using another separate profile at the edge of an already excavated portion of the area to calibrate the resistivity values with soil types. Each line consisted of 41 stainless steel electrodes at 0.5 m minimum spacing, connected to two smart cables each with 21 take-outs, using jumpers. Pole-dipole electrode array arrangement with its high penetration depth at relatively small electrode spacing was used for data acquisition. Multi-electrode resistivity metre (ABEM Terrameter SAS4000 system, Guideline Geo AB, Sweden) was used for the measurements upon administering a specific amount of current (20 mA). The system selects the four active electrodes for each voltage measurement automatically and computes the apparent resistivity. Standard constrained least-square inversion was applied to the apparent resistivity data using Res2Dinv software package to develop the 2-D (true) resistivity of the subsurface. Contours of true resistivity datasets were plotted using Surfer 8 software package to build the true subsurface resistivity tomograms. Resistivity values obtained from the calibration line were grouped according to the subsurface soil types to serve as a control for interpreting the tomograms obtained from the ten profiles (L1-L10). The survey layout with location of the calibration line (CL) and the ten profiles (L1-L10) is shown in Figure 4.

RESULTS AND DISCUSSION

Results obtained from the resistivity profiles suggested four resistivity groups; very-low resistivity (< 20 Ωm), low resistivity (20-100 Ωm), intermediate resistivity (100-200 Ωm) and high resistivity (> 200 Ωm). Figure 5 shows an electrical resistivity tomogram obtained from the calibration line (CL), together with the cross section of an excavated portion of the study area. Figure 5(a) reveals three distinct subsurface layers, namely sandy clay, sandy clay mixed with shell flakes, and sand. These layers correlate with resistivity values obtained at the excavated portion: 50-100 Ωm for sandy clay, 100-200 Ωm for sandy clay mixed with shell flakes and > 200 Ωm for sand (Figure 5(b)). A summary of resistivity groups with soil types is shown in Table 2.

Maejo Int. J. Sci. Technol. **2020**, *14*(02), 119-129

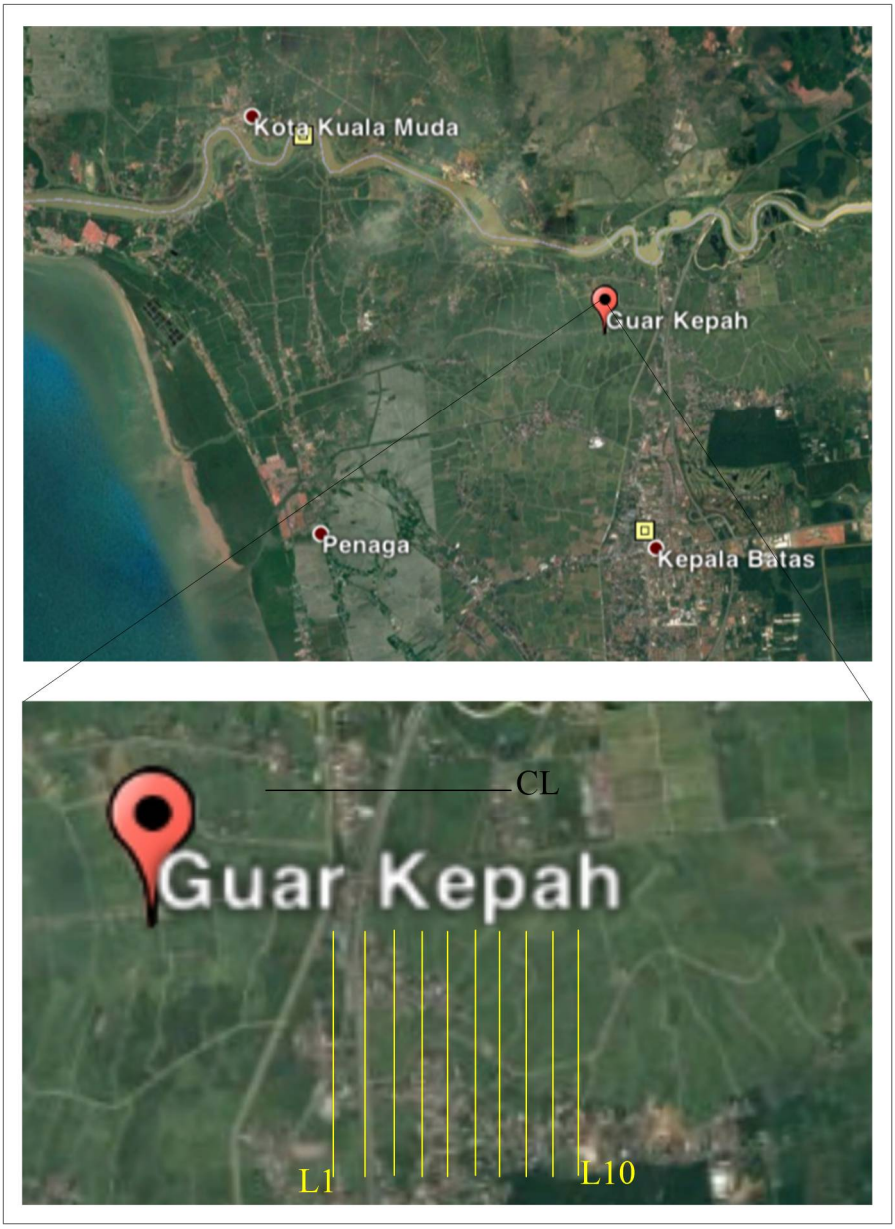

Figure 4. Survey layout (Google Earth)

The very-low resistivity layer (first group) was not identified in the subsurface layers in Figure 5. However, the presence of clay in the area (Figure 5(a)) suggested that a very-low resistivity group might exist in the form of wet clay. Therefore, the resistivity group of less than 20 Ωm was assumed to be wet clay as the value did not differ much from that for sandy clay. The values obtained also agree with the theoretical values (Table 1).

Figure 6 shows resistivity tomograms obtained from the ten profiles (L1-L10). It can be observed from the figure that an anomaly (indicated by a rectangular box) exists at the right side of all ten tomograms at about the same location. The anomaly reflects a material of very low resistivity (< 20 Ωm) surrounded by a high-resistivity material (> 200 Ωm), which is interpreted as wet clay surrounded by sand. Appearance of the anomaly in all the ten consecutive tomograms suggests the presence of an artefact of non-uniform dimension. Another similar anomaly (indicated by a dash

Maejo Int. J. Sci. Technol. **2020**, *14*(02), 119-129

box) can be observed at the left side of profiles L3 and L4 and can be interpreted in the same fashion since they are of the same resistivity range at about the same depth.

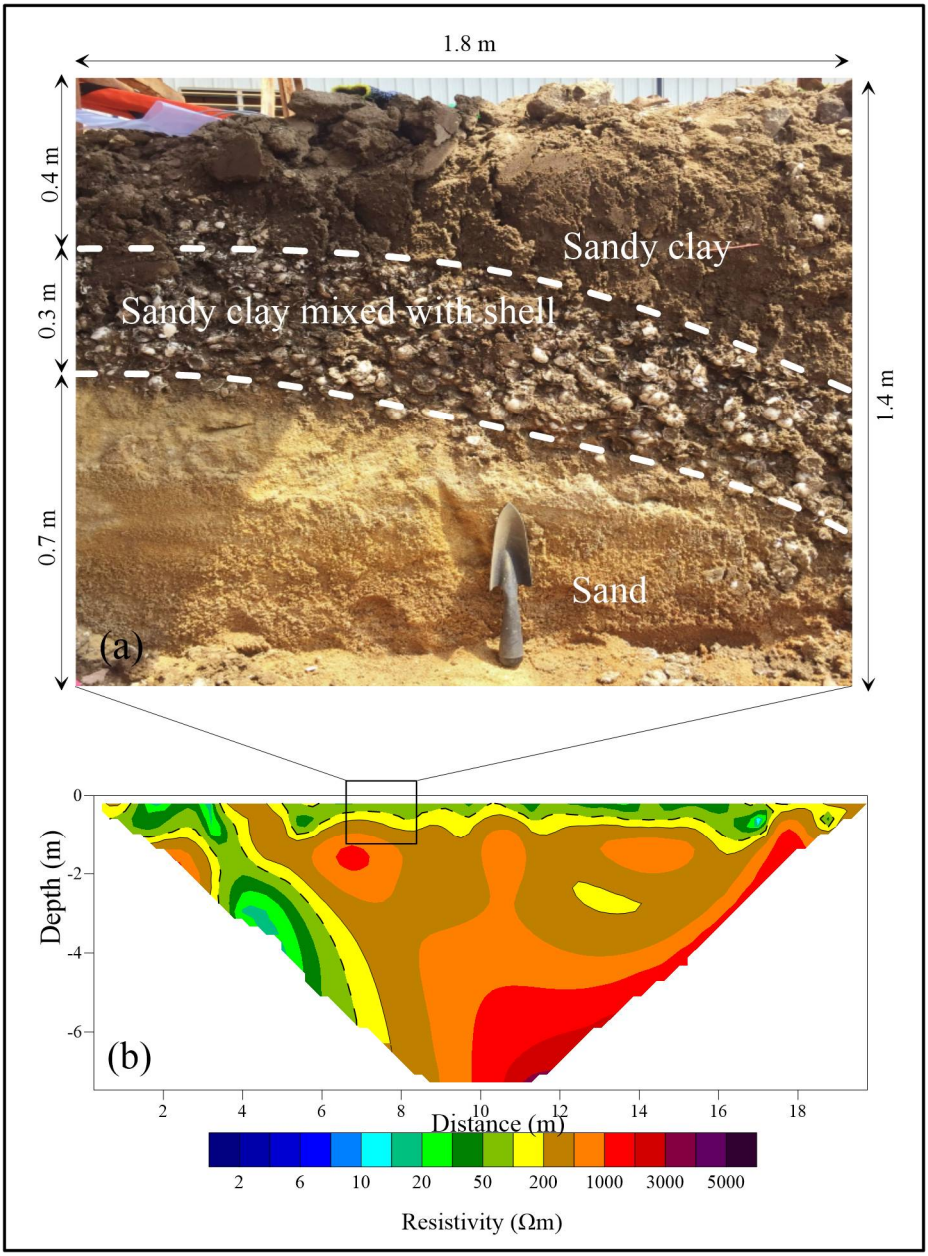

Figure 5. Resistivity tomogram from calibration line (CL) at the edge of an excavated area

Table 2. Summary of resistivity groups with soil types

Resistivity group	Resistivity range (Ωm)	Soil type
Very low resistivity	< 20	Clay
Low resistivity	20-100	Sandy clay
Intermediate resistivity	100-200	sandy clay + shell
High resistivity	> 200	Sand

A few other anomalies of very low resistivity (< 20 Ωm) exist in the remaining tomograms although they are generally of smaller dimensions and do not show any clear pattern or consistency.

Maejo Int. J. Sci. Technol. **2020**, *14*(02), 119-129

Hence they are not regarded as indicating any meaningful objects. They may probably be false anomalies arising from the inversion process. The presence of green to yellow colours within the boxes, which may ordinarily indicate low to intermediate resistivity groups, does not signify the presence of shell in the marked portions. They may be due to the smearing effect of abrupt transition from very low resistivity to high resistivity or vice versa. This is typical of most inversion processes.

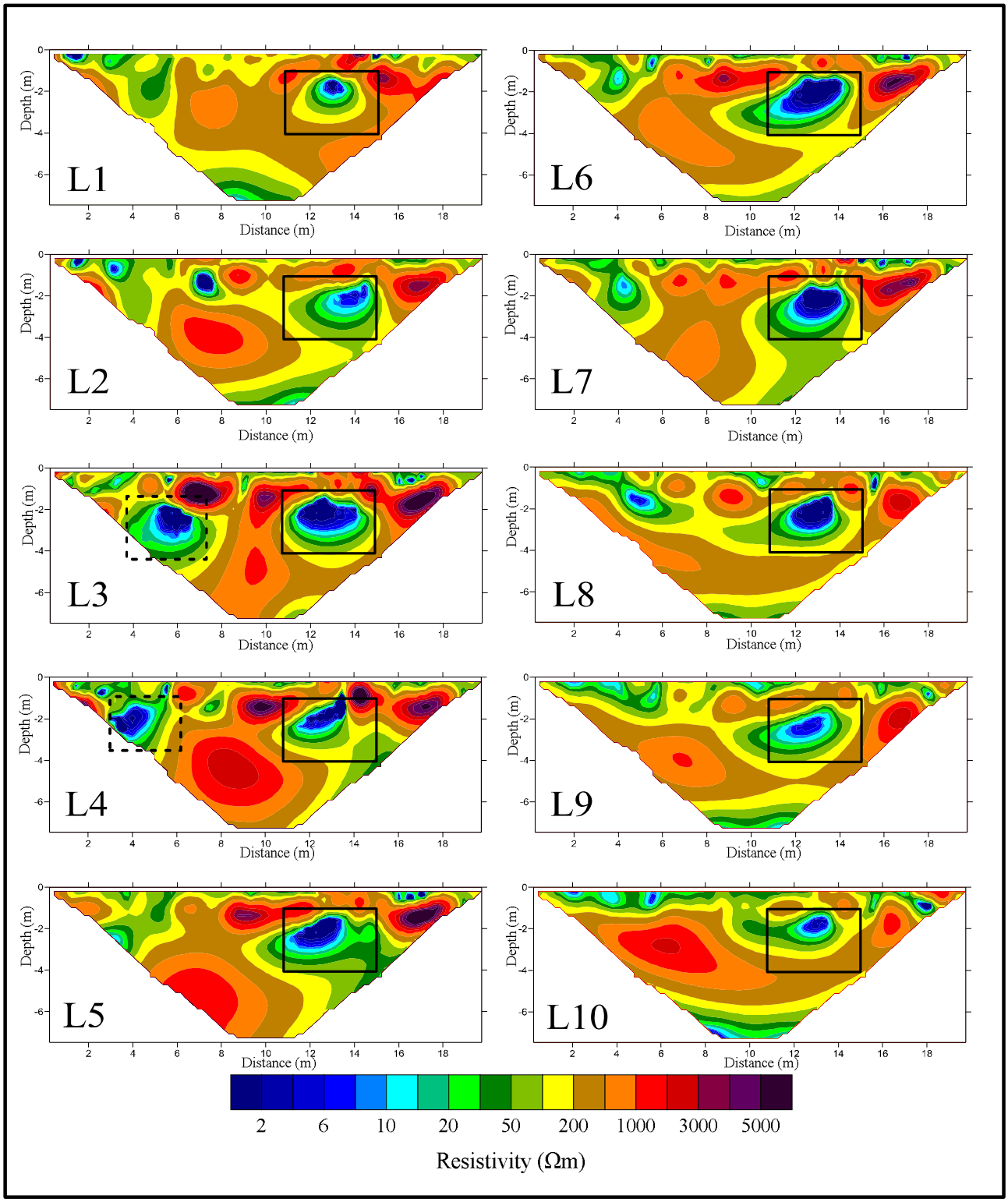

Figure 6. Resistivity tomograms along ten profiles L1-L10

Maejo Int. J. Sci. Technol. **2020**, *14*(02), 119-129

CONCLUSION

The study has successfully characterised the different soil types of the subsurface soil at Guar Kepah, Kedah Tua, an important archaeological site of Malaysia.

ACKNOWLEDGEMENTS

The authors wish to thank Centre for Global Archaeological Research, Universiti Sains Malaysia for funding this research with Grant 304/PARKEO/650894/K104 and the staff and postgraduate students of Geophysics Section, School of Physics, Universiti Sains Malaysia for their efforts during the data acquisition.

REFERENCES

1. J. M. Reynolds, "An Introduction to Applied and Environmental Geophysics", 2nd Edn., John Wiley and Sons, Chichester, **1997**, Ch.7.
2. M. Moorkamp, A. W. Roberts, M. Jegen, B. Heincke and R. W. Hobbs, "Verification of velocity-resistivity relationships derived from structural joint inversion with borehole data", *Geophys. Res. Lett.*, **2013**, *40*, 3596-3601.
3. R. Dalan, J. Sturdevant, R. Wallace, B. Schneider and S. De. Vore, "Cutbank geophysics : A new method for expanding magnetic investigations to the subsurface using magnetic susceptibility testing at Awatixa Hidatsa Village, North Dakota", *Remote Sens.*, **2017**, *9*, Art. no.112.
4. F. J. Davey, "New Zealand geophysical observatories 1862-1931", *J. R. Soc. New Zealand*, **2017**, *47*, 80-87.
5. R. Saad, N. A. Ismail, M. M. Nordiana and M. Saidin, "The conclusion of searching Bukit Bunuh crater using gravity method", *Electron. J. Geotech. Eng.*, **2014**, *19*, 4383-4392.
6. S. Wada, A. Sawada, Y. Hiramatsu, N. Matsumoto, S. Okada, T. Tanaka and R. Honda, "Continuity of subsurface fault structure revealed by gravity anomaly : The eastern boundary fault zone of the Niigata plain, central Japan", *Earth Planets Space*, **2017**, *69*, Art. no.15.
7. A. Ebrahimi, A. Gholami and M. Nabi-Bidhendi, "Sparsity-based GPR blind deconvolution and wavelet estimation", *J. Indian Geophys. Union*, **2017**, *21*, 7-12.
8. S. Yao, M. Wang, S. Duan, S. Chen, W. Liu and D. Xu, "Exploring sandstone body in weak electrical resistivity contrast with AMT data", *Int. J. Geosci.*, **2017**, *8*, 277-285.
9. W. M. Telford, L. P. Geldart and R. E. Sheriff, "Resistivity methods", in "Applied Geophysics", 2nd Edn. (Ed. W. M. Telford, L. P. Geldart and R. E. Sheriff), Cambridge University Press, New York, **1990**, Ch.8.
10. A. A. Bery and R. Saad, "Tropical clayey sand soil's behaviour analysis and its empirical correlations via geophysics electrical resistivity method and engineering soil characterizations", *Int. J. Geosci.*, **2012**, *3*, 111-116.
11. A. Abdulrahman, M. N. M. Nawawi, R. Saad and K. A. N. Adiat, "Volumetric assessment of leachate from solid waste using 2D and 3D electrical resistivity imaging", *Adv. Mater. Res.*, **2013**, *726*, 3014-3022.
12. M. Syukri, R. Saad and M. Abubakar, "Leachate migration delineation using 2-D electrical resistivity imaging (2-D ERI) at Gampong Jawa, Banda Aceh", *Electron. J. Geotech. Eng.*, **2013**, *18*, 1505-1510.

13. U. Massoud, M. Soliman, A. Taha, A. Khozym and H. Salah, "1D and 3D inversion of VES data to outline a fresh water zone floating over saline water body at the northwestern coast of Egypt", *NRIAG J. Astron. Geophys.*, **2015**, *4*, 283-292.
14. J. E. Chambers, P. B. Wilkinson, D. Wardrop, A. Hameed, I. Hill, C. Jeffrey, M. H. Loke, P. I. Meldrum, O. Kuras, M. Cave and D. A. Gunn, "Bedrock detection beneath river terrace deposits using three-dimensional electrical resistivity tomography", *Geomorphol.*, **2012**, *177-178*, 17-25.
15. C. Vachiratienchai and W. Siripunvaraporn, "An efficient inversion for two-dimensional direct current resistivity surveys based on the hybrid finite difference – finite element method", *Phys. Earth Planet. Inter.*, **2013**, *215*, 1-11.
16. N. Ali, R. Saad and M. M. Nordiana, "Integration of seismic refraction and 2D electrical resistivity in locating geological contact", *Open J. Geol.*, **2013**, *3*, 7-12.
17. R. Saad, M. M. Nordiana and M. Saidin, "Resistivity studies of archaeological anomaly at Sungai Batu, Lembah Bujang, Kedah (Malaysia)", *Electron. J. Geotech. Eng.*, **2014**, *19*, 2589-2596.
18. R. Yusoh, R. Saad, M. Saidin, S. B. Muhammad, S. T. Anda, M. A. M. Ashraf and Z. A. M. Hazreek, "Visualizing Sungai Batu ancient river, Lembah Bujang archaeology site, Kedah – Malaysia using 3-D resistivity imagining" *J. Phys.*, **2018**, *995*, Art. no. 012117.
19. M. Jinmin, R. Saad, M. M. Nordiana, S. B. Muhammad and S. Mokhtar, "3-D resistivity imaging on archaeology characterization at Sungai Batu area in Kedah, Malaysia", *Mater. Sci. Eng.*, **2017**, *226*, Art. no.012047.
20. D. F. Rucker, N. Crook, D. R. Glaser and M. H. Loke, "Pilot-scale field validation of the long electrode electrical resistivity tomography method", *Geophys. Prospect.*, **2012**, *60*, 1150-1166.
21. M. H. Loke, H. Kiflu, P. B. Wilkinson, D. B. Harro and S. Kruse, "Optimized arrays for 2D resistivity surveys with combined surface and buried arrays", *Near Surf. Geophys.*, **2015**, *13*, 505-517.
22. T. Ingeman-Nielsen, S. Tomaškoviová and T. Dahlin, "Effect of electrode shape on grounding resistances – Part 1: The focus-one protocol", *Geophys.*, **2016**, *81*, 159-167.
23. S. B. Muhammad, R. Saad, M. Saidin, R. Yusoh, T. A. Sabrian and Y. M. Samuel, "Internal architecture of meteorite impact crater at Bukit Bunuh, Lenggong – Perak, Malaysia inferred from upward continuation of magnetic field intensity data", *J. Phys.*, **2018**, *995*, Art.no. 012092.
24. T. A. Sabrian, R. Saad, M. Saidin, S. B. Muhammad, and R. Yusoh, "Empirical approach in developing Vs/Vp ratio for predicting S-wave velocity, study case; Sungai Batu, Kedah", *J. Phys.*, **2018**, *995*, Art.no.012089.
25. Y. M. Samuel, R. Saad, N. M. Mustaza, M. Saidin and S. B. Muhammad, "Integration of magnetic and geotechnical methods shallow subsurface soil characterization at Sungai Batu, Kedah, Malaysia", *J. Phys.*, **2018**, *995*, Art.no.012090.
26. R. Yusoh, R. Saad, M. Saidin, S. T. Anda, S. B. Muhammad, M. I. M. Ashraf and Z. A. M. Hazreek, "Optimization of archaeological anomalies using GIS method for magnetic and resistivity study at Sungai Batu, Lembah Bujang, Kedah (Malaysia)", *J. Phys.,* **2018**, *995*, Art. no. 012072.
27. N. Rahman, N. A. Ismail and S. Mokhtar, "Shell mound investigation at Guar Kepah (Penang, Malaysia) using 2-D resistivity imaging for archaeological study ", *J. Phys. Sci.*, **2019**, *30*, 17-23.

Maejo Int. J. Sci. Technol. **2020**, *14*(02), 119-129

28. H. D. Tjia, "Ancient shorelines in Peninsular Malaysia", Proceedings of SPAFA Seminar in Prehistory of Southeast Asia, **1987**, Bangkok, Thailand, pp.239-257.
29. D. B. Courtier, "Geology and Mineral Resources of the Neighbourhood of Kulim, Kedah", Ministry of Primary Industries, Kuala Lumpur, **1974**, pp.1-49.
30. K. bin Hassan, "A summary of the Quaternary geology investigations in Seberang Prai, Pulau Pinang and Kuala Kurau", *Geol. Soc. Malaysia Bull.*, **1990**, *26*, 47-53.
31. W. Lowrie, "Fundamentals of Geophysics" 2nd Edn., Cambridge University Press, Cambridge, **2007**, pp.256-261.